1-24-2018

Nonreciprocal Localization of Photons

Hamidreza Ramezani

Pankaj K. Jha

Yuan Wang

Xiang Zhang

Recommended Citation

Hamidreza Ramezani, et. al., (2018) Nonreciprocal Localization of Photons.Physical Review Letters120:4. DOI: http://doi.org/10.1103/PhysRevLett.120.043901

Non-reciprocal Localization of Photons

Hamidreza Ramezani[1,2], Pankaj K. Jha[1], Yuan Wang[1], Xiang Zhang[1*]
[1] *NSEC, University of California, Berkeley, 3112 Etcheverry Hall, Berkeley, CA 94720, USA and*
[2] *Department of Physics and Astronomy, University of Texas Rio Grande Valley, Brownsville, TX 78520, USA (current)*

We demonstrate that it is possible to localize photons non-reciprocally in a moving photonic lattice made by spatiotemporally modulating the atomic response, where the dispersion acquires a spectral Doppler shift with respect to the probe direction. A static defect placed in such a moving lattice produces a spatial localization of light in the bandgap with a shifting frequency that depends on the direction of incident field with respect to the moving lattice. This phenomenon has an impact not only in photonics but also in broader areas such as condensed matter and acoustics, opening the doors for designing new devices such as compact isolators, circulators, non-reciprocal traps, sensors, unidirectional tunable filters, and possibly even a unidirectional laser.

PACS numbers:

Artificial defects embedded in periodic structures are an important foundation for creating localized modes and producing localized resonant modes in the gap[1, 2]. Thus such defects are good candidates for designing photonic crystal lasers[3–6] and they have vast range of applications such as strain field traps[7], strong photon localization[8], mode selection[9], and lasers[3–5, 10, 11] to name a few. While full domination of the wave propagation requires controlling the directionality [12–14], up to now all the proposed localized modes have been reciprocal and restricted by time reversal symmetry.

Consequently, localization is bidirectional and photons in the forbidden stop band are confined irrespective of the direction of the incident beam. Furthermore, while in photonic crystals modulation occurs in the real part of the refractive index, recently parity-time symmetric systems have been proposed where the imaginary part of the index is periodically altered. Asymmetric reflections in 1D parity-time symmetric structures have been proposed as a method for creating unidirectional, yet reciprocal, transports such as unidirectional invisibility[15], unidirectional lasing[16, 17] and unidirectional anti-laser[18]. However, in all the aforementioned phenomena in the absence of the magnetic effect, in Hermitian and non-Hermitian systems, the band structure is symmetric and any non-reciprocal light propagation is prohibited. Specifically, lattices with time symmetry or more precisely any symmetry that changes the wavevector k to $-k$ do not support asymmetric band structure[19]. Consequently, the transmitted field in such lattices is symmetric and independent of the input channel. Nevertheless, in recent years there is a demand for non-reciprocal transport, especially in miniaturized and compact systems[20–23].

Magnetic biasing, for example in Faraday isolators, is the most common technique to break the reciprocity[24, 25]. In a similar fashion, a periodic stack of anisotropic dielectrics and gyrotropic magnetic layers results in asymmetric band structures[13, 19, 20]. More recently, one-way frequency conversion in waveguides has been proposed by means of spatiotemporally modulated index of refraction[12] which results in magnetic-free non-reciprocal optical [21, 22], acoustic[26, 27], and radio-frequency[28] transport where a temporal potential imitates a magnetic field responsible for non-reciprocity[29–31].

Here we propose a non-reciprocal localized defect mode at a specific frequency. Specifically, the non-reciprocal trapping of light results in the unidirectional exponential accumulation of photons traveling in only one direction. For a finite system, such localized modes result in non-zero transmission in the bandgap. In the opposite direction and at the same frequency, photons end up in the bandgap and thus their propagation is forbidden. For a reasonably strong modulation we show that one can obtain an interesting situation, wherein one direction photons get trapped, namely localized, while in the opposite direction and at the same frequency the photons are in the passband with scattering mode feature. Particularly in a scattering mode, unlike the localized mode, the field does not have exponential form. Finally, we show the frequency shift of the defect mode is linearly proportional to the detuning similar to the Zeeman effect. The non-reciprocal defect mode can filter the unwanted frequencies in the bandgap and transmit the defect mode signal. By changing the detuning one can tune the filtering frequency in a nonreciprocal manner.

To realize a non-reciprocal localized mode, as schematically depicted in Fig. (1), we embed a defect in a periodic spatiotemporally modulated 1D lattice. Although our proposal is general and can be implemented in different wave-base systems, we consider a periodic photonic lattice generated in a three-level electromagnetically-induced-transparency (EIT) medium. The three-level system we consider (see the left inset of Fig.1), has a typical Λ-configuration with upper level $|a\rangle$ $(P_{3/2}, F = 1)$ and two lower-levels $|b\rangle$ $(S_{1/2}, F = 1)$ and $|c\rangle$ $(S_{1/2}, F = 2)$, where $|a\rangle \leftrightarrow |b\rangle$ and $|a\rangle \leftrightarrow |c\rangle$ are allowed dipole transitions while transition $|c\rangle \leftrightarrow |b\rangle$ is forbidden due to parity selection rule. The coupling

fields $\mathbf{E}_c(t) = \frac{\hat{y}}{2}\left\{\mathcal{E}_1 e^{i(\mathbf{k}_1\cdot\mathbf{r}-\omega_1 t)} + \mathcal{E}_2 e^{i(\mathbf{k}_2\cdot\mathbf{r}-\omega_2 t)} + \text{c.c}\right\}$ drive the transition $|a\rangle \leftrightarrow |c\rangle$ with atomic transition frequency ω_{ac}. The weak probe field $\mathbf{E}_p(t) = \frac{\hat{y}}{2}\left\{\mathcal{E}_f(z,t)e^{i(\mathbf{k}_f\cdot\mathbf{r}-\omega_f t)} + \mathcal{E}_b(z,t)e^{i(\mathbf{k}_b\cdot\mathbf{r}-\omega_b t)} + \text{c.c}\right\}$ excites the transition, $|a\rangle \leftrightarrow |b\rangle$ with atomic transition frequency ω_{ab}. In the limit of $\mathcal{E}_{1,2} \gg \mathcal{E}_{b,f}$, we can approximately assume all the populations reside in level $|b\rangle$ and we obtain the equations of motion for the coherences ρ_{ij}

$$\begin{aligned}\frac{d\rho_{ab}}{dt} &= -\Gamma_{ab}\rho_{ab} + i\left[\Omega_f e^{i\mathbf{k}_f\cdot\mathbf{r}} + \Omega_b e^{i\mathbf{k}_b\cdot\mathbf{r}} e^{i\Delta t}\right] e^{-i\omega_f t} + \\ &\quad i\left[\Omega_1 e^{i\mathbf{k}_1\cdot\mathbf{r}} + \Omega_2 e^{i\mathbf{k}_2\cdot\mathbf{r}} e^{-i\delta t}\right] e^{-i\omega_1 t}\rho_{cb} \\ \frac{d\rho_{cb}}{dt} &= -\Gamma_{cb}\rho_{cb} + i\left[\Omega_1^* e^{-i\mathbf{k}_1\cdot\mathbf{r}} + \Omega_2^* e^{-i\mathbf{k}_2\cdot\mathbf{r}} e^{i\delta t}\right] e^{i\omega_1 t}\rho_{ab}\end{aligned} \tag{1}$$

Above, the Rabi-frequencies are $\Omega_{1,2} = (\wp_{ac}\cdot\hat{y}/2)\,\mathcal{E}_{1,2}$, $\Omega_{b,f} = (\wp_{ab}\cdot\hat{y}/2)\,\mathcal{E}_{b,f}$, the detunings are $\delta = (\omega_2 - \omega_1)$, $\Delta = (\omega_f - \omega_b)$ and the decay of optical coherences are $\Gamma_{ab} = (i\omega_{ab} + \gamma_{ab})$, $\Gamma_{cb} = (i\omega_{cb} + \gamma_{cb})$. We seek solutions of the form $\rho_{ij} = \sum_n \sigma_{ij}^{[n]} \exp\left[i(\Delta\mathbf{k}_{ij}^{[n]}\cdot\mathbf{r} - \omega_{ij}^{[n]}t)\right]$ where $\Delta\mathbf{k}_{ij}^{[n]}$ is the n^{th} order wavevector mismatch. Considering that the counter-propagating coupling fields and the forward probe field are along the z-direction, the reflected field will be generated in the backward direction via phase-matching condition $\Delta = -\delta$ and its frequency (for left incident beam, namely toward $+z$) is $\omega_b = \omega_f + \delta$. From the solution of Eq. (1) one can obtain the zeroth-order and the first-order terms of the coherence as $\sigma_{ab}^{[0]} = uA_0 + v\tilde{A}_1$, and $\sigma_{ab}^{[1]} = u^{'}A_0 + v^{'}\tilde{A}_1$ where the coefficients are defined as $u = \left[\alpha_0 - \left(\frac{\gamma_1\beta_0}{\alpha_1 - \beta_1\zeta_2}\right) - \left(\frac{\gamma_0\beta_{-1}}{\alpha_{-1} - \gamma_{-1}\xi_2}\right)\right]^{-1}$, $v = \left(\frac{\beta_0}{\alpha_1 - \beta_1\zeta_2}\right)u$, $u^{'} = \frac{\gamma_1 u}{\alpha_1 - \beta_1\zeta_2}$, $v^{'} = \frac{1+\gamma_1 v}{\alpha_1 - \beta_1\zeta_2}$ and $\alpha_n = 1 - B_n D_n - C_n E_{n-1}$, $\beta_n = B_n E_n$, $\gamma_n = C_n D_{n-1}$, $\zeta_n = \sigma_{ab}^{[n]}/\sigma_{ab}^{[n-1]}$ (for $n \neq 0{,}1$), $\xi_n = \sigma_{ab}^{[-n]}/\sigma_{ab}^{[-(n-1)]}$ (for $n \neq 0{,}1$). Moreover, the coefficients that quantify the atomic parameters are defined as $A_n = \frac{i\Omega_f}{-i\Delta_f + \gamma_{ab} - in\delta}$, $\tilde{A}_n = \frac{i\Omega_b e^{-i\Delta kz}}{-i\Delta_f + \gamma_{ab} - in\delta}$, $E_n = \frac{i\Omega_2^*}{-i\Delta_f + \gamma_{cb} - in\delta}$, $B_n = \frac{i\Omega_1}{-i\Delta_f + \gamma_{ab} - in\delta}$, $C_n = \frac{i\Omega_2}{-i\Delta_f + \gamma_{ab} - in\delta}$, $D_n = \frac{i\Omega_1^*}{-i\Delta_f + \gamma_{cb} - in\delta}$. Here we have defined the detunings as $\Delta_{f,b} \equiv \omega_{f,b} - \omega_{ab}$. Propagation of the probe field is given by the Maxwell's wave equation

$$\frac{\partial^2 E_p}{\partial z^2} - \frac{1}{c^2}\frac{\partial^2 E_p}{\partial t^2} = \mu_0\frac{\partial^2 P}{\partial t^2} \tag{2}$$

where the polarization in the EIT medium and the defect takes the form $P = N\wp_{ba}\rho_{ab}(z,t) + \text{c.c}$ and $P = 0$, respectively. As noted earlier, only the zeroth-order and the first-order terms are dominant in the coherence term ρ_{ab}. Subsequently, within slowly varying envelope approximation, Eq.(2) yields (in steady-state) the Schrödinger-like coupled mode equation for the weak forward and backward traveling fields generated by the probe in the spatiotemporal modulated medium

$$i\frac{d}{dz}\vec{\psi} = \begin{pmatrix} \kappa_{11}(\omega_f) & \kappa_{12}(\omega_b)e^{-i\Delta kz} \\ \kappa_{21}(\omega_f)e^{i\Delta kz} & \kappa_{22}(\omega_b)\end{pmatrix}\vec{\psi} \tag{3}$$

where $\vec{\psi} = \begin{pmatrix}\Omega_f & \Omega_b\end{pmatrix}^T$. The off-diagonal terms in the 2×2 matrix mix the waves while the diagonal ones are attenuation coefficients associated with the probe field with frequency ω_f propagating in the z direction, namely $\kappa_{21(12)} = (-)\theta_{b(f)}\left(\frac{u^{'}(v)}{\gamma_{ab} - i\Delta_{f(b)}}\right)$, and $\kappa_{22(11)} = (-)\theta_{b(f)}\left(\frac{v^{'}(u)}{\gamma_{ab} - i\Delta_{b(f)}}\right)$ where $\theta_{f,b} = \frac{N|\wp_{ab}|^2 k_{f,b}}{2\hbar\epsilon_0}$. Notice that the field propagation in a time-dependent spatially modulated waveguide system is described by a similar equation [12]. Below, we assume the EIT medium is composed of cold rubidium atoms distributed homogeneously in a cell of about 2mm length which has two parts separated by a SiN dielectric membrane (defect) with 88.6nm length and refractive index $n = 2.2 + 10^{-4}i$.

Solving differential equations (2) and (3) simultaneously and using the transfer matrix method we can calculate the transmission (T) and reflection (R) from our moving photonic crystal. Figure (2a) depicts the transmission and reflection coefficients vs. probe detuning Δ_f in the presence of the membrane and the detuning δ (normalized with respect to decoherence rate between levels $|a\rangle \leftrightarrow |b\rangle$; γ_{ab}) and with $\omega_{ab} \approx 2414191.334$ GHz. In the absence of the membrane, the spatial periodicity of the dielectric constant of the photonic crystal generates a Bragg reflection where photon propagation is forbidden in a window known as the bandgap. Thus, in the bandgap the transmission coefficient drops to zero. Considering the intrinsic losses in the system at the photonic bandgap the reflection plus absorption sum to one. As depicted in Fig.(2a) by inserting the membrane into the cell, a defect mode with non-zero transmission appears in the bandgap at $\Delta_f \approx -0.12$MHz. We highlighted the position of this mode with an arrow. Such a defect mode is a bound state out of continuum and is created due to the resonances.

The transmission peak of the defect mode is reciprocal and *degenerate*, namely, irrespective of the direction of the incident field the transmission peak occurs at the same frequency. When we introduce a nonzero detuning, i.e. the permittivity of the photonic lattice becomes both space- and time-dependent, degeneracy breaks and the frequency of the defect mode associated with the left and right incident beams becomes different. Neglecting the higher quasi energies, we plotted left incident transmission and reflection in the figure (2b) for $\delta = 0.015\gamma_{ab}$. In this case, the defect mode appears at the probe detuning $\Delta_f \approx -0.37$MHz (see the green dash line). On the other hand, in figure (2c) we observe that for the right incident field the defect mode appears at $\Delta_f \approx -0.28$MHz (orange dash line).

The transmission and reflection peaks at the defect mode have a sharp feature in the absence of the losses. At the defect state, photons are trapped and the electric field is localized around the membrane. Specifically, the electric field envelope decays exponentially as we move away from the defect. This contrasts with the resonant peaks at the scattering states where the field is distributed all over the photonic crystal. In our photonic lattice a comparison between Fig.(2a) and Fig. (2b,c) shows that due to the time-dependent modulation position and width of the bandgap window vary when the detuning is chenged and at the same time it affects the position of the localized modes. To distinguish the localized mode from the scattering modes one should plot the field distribution for the localized mode. As long as the field has an exponential form we have the trapping of photons. However, eventually for very strong detuning, the mode will completely merge with the band and its associated field distribution will not have an exponential shape. Specifically, one can use detuning to tune the mode from being completely localized to a non-localized one. In figures (3a-i) we plotted the field distribution in the photonic crystal for different detuning and at different probe detuning. Specifically, in Figs.(3a-c) we plotted the field at $\Delta_f = -0.1179$MHz (localized mode with exponential form), $\Delta_f = -0.2162$MHz (scattering mode), and $\Delta_f = -0.5$MHz (a mode in the bandgap) for $\delta = 0$. We clearly observe the difference in the field distribution in each case. To compare the field distribution for non-zero detuning we plotted the field for the left and right incident beams at $\Delta_f = -0.389$MHz, $\Delta_f = -0.282$MHz, and $\Delta_f = -0.155$MHz for $\delta = 0.015\gamma_{ab}$ in Figs.(3d-f) and Figs.(3g-i), respectively. In all cases for the defect mode, the exponential decay around the membrane is clearly observed. It is interesting that for $\Delta_f = -0.389$MHz the photons coming from the left side will be localized while for the same photons coming from the right they will be in the bandgap and get reflected. However, for $\Delta_f = -0.282$MHz the photons coming from the right will be localized and photons with the same frequency coming from the left side will be in the band and form a scattering mode with finite transmission and reflection.

As discussed previously the nonzero detuning between the counterpropagating fields splits the defect modes associated with the left and right incident beams. The splitting is linear with respect to the detuning similar to the Zeeman effect where a magnetic field splits the degenerate modes. This similarity between time-dependent potentials and the magnetic field is the basic principle behind the breaking of the Lorentz reciprocity. However, to the best of our knowledge there is no report on the existence of non-reciprocal localized mode based on magnetic effects. We mentioned earlier that the frequency of the localized mode is linearly dependent on the detuning. In Figure (4) we numerically calculated the changes in the frequency of the localized modes for the left and right incident fields versus the detuning. A linear fitting shows that our anticipation is correct and it behaves linearly similar to the Zeeman effect.

Any type of isolator based on magnetic field or time-dependent modulation needs an absorbing and/or filtering channel to remove the undesired signal. Otherwise, in the absence of the filtering channel, the undesired field will be able to pass through the isolator after several forward and backward propagations. Our proposal is not distinct in this sense. However, in our case, the undesired signal is in the gap and needs to travel several times to be able to pass through our proposed isolator. For example, let us consider the case represented in Fig.(2b,c) and assume that we lunch a signal from the left with frequency associated with the defect mode, namely at $\Delta_f = -0.38$. Thus, the left incident signal can pass the lattice. On the other hand if a similar signal comes from the right, it will not pass the lattice and gets reflected at the frequency $\omega_b = \omega_f - \delta$. This process will continue $n(= \frac{|\Delta_f^{\text{passband before the gap}} - \Delta_f^{\text{defect}}|}{\delta} \approx \frac{|-0.9+0.39|}{0.09} \approx 5)$ times until the frequency of the reflected signal decreases to the value which belongs to the passband frequency just before the bandgap. We mentioned earlier that naturally, there are some intrinsic distributed losses in our optical system. Consequently, the undesired signal coming from the right side observes the intrinsic losses n times more. Thus, our proposal is more compact with respect to the other isolators.

In conclusion, we have shown that by embedding a defect in spatiotemporally periodic modulated photonic lattice one can achieve a non-reciprocal defect mode where the photons propagating in one direction become localized and get trapped in the bandgap, while in the opposite direction photons with the same frequency get reflected or transmitted depending on the position of the mode in the bandgap window. This contrasts with the periodic spatial modulated case where a defect generates a reciprocal defect mode. Moreover, we showed that the position of the defect mode is tunable and depends on the strength of the temporal modulation. Specifically, the position of the defect mode linearly changes with respect to the temporal modulation. Our proposal can have application in designing compact isolators, circulators, unidirectional sensors and filters. Of great interest will be extending non-reciprocal localized mode to non-Hermitian defects such as a gain or loss medium embedded in the lattice which might lead to unidirectional lasing or absorption.

Acknowledgments – H. R acknowledge funding support from the UT system under the Valley STAR award. H.R. conceived the idea and performed analytical and numerical calculation associated with the transfer matrix, P. K. J. performed the atomic analytical and numerical calculations. X.Z. and Y.W. guided the research. All authors contributed to discussions and wrote the Letter.

* Electronic address: xiang@berkeley.edu

[1] Y. Akahane, T. Asano, B.-S. Song, and S. Noda, Nature 425, 944-947 (2003).
[2] B.-S. Song, S. Noda, T. Asano, and Y. Akahane, Nat. Mater. 4, 207-210 (2005).
[3] O. Painter, R. K. Lee, A. Scherer, A. Yariv, J. D. ÓBrien, P. D. Dapkus, I. Kim, Science 284, 5421, pp. 1819-1821(1999).
[4] K. Zhong, *et al.*, ACS Photonics 3 (12), pp 2330-2337 (2016).
[5] R. Colombelli, *et al.*, Science 302, 1374 (2003).
[6] S. Noda, M. Yokoyama, M. Imada, A. Chutinan, and M. Mochizuki, Science 293, 1123 (2001).
[7] A. J. Sievers and S. Takeno, Phys. Rev. Lett. 61, 970 (1988).
[8] S. John, Phys. Rev. Lett. 58, 2486 (1987).
[9] C. Poli, M. Bellec, U. Kuhl, F. Mortessagne, and H. Schomerus, Nat. Commun. 6, 6710 (2015).
[10] H.-G. Park, *et al.*, Science 305, 1444 (2004).
[11] B. Ellis, M. A. Mayer, G. Shambat, T. Sarmiento, J. Harris, E. E. Haller, and J. Vukovi, Nat. Photonics 5, 297 (2011).
[12] Z. Yu and S. Fan, Nat. Photonics 3, 91 (2009).
[13] H. Ramezani, Z. Lin, S. Kalish, T. Kottos, V. Kovanis, and I. Vitebskiy, Opt. Express 20, 26200 (2012).
[14] H. Ramezani, T. Kottos, R. El-Ganainy, and D. N. Christodoulides, Phys. Rev. A 82, (2010).
[15] Z. Lin, H. Ramezani, T. Eichelkraut, T. Kottos, H. Cao, and D. Christodoulides, Phys. Rev. Lett. 106 (21), 213901, (2011).
[16] H. Ramezani, S. Kalish, I. Vitebskiy, and T. Kottos, Phys. Rev. Lett. 112, 043904, (2014).
[17] H. Ramezani, H.-K. Li, Y. Wang, and X. Zhang, Phys. Rev. Lett. 113, (26), 263905 (2014).
[18] H. Ramezani, Y. Wang, E. Yablonovitch, and X. Zhang, IEEE J. Sel. Top. Quantum Electron. 22, 115 (2016).
[19] A. Figotin and I. Vitebsky, Phys. Rev. E 63, 066609 (2001).
[20] L. Bi, J. Hu, P. Jiang, D. H. Kim, G. F. Dionne, L. C. Kimerling, and C. A. Ross, Nat. Photonics 5, 758 (2011).
[21] H. Lira, Z. Yu, S. Fan, and M. Lipson, Phys. Rev. Lett. 109, (2012).
[22] D.-W. Wang, H.-T. Zhou, M.-J. Guo, J.-X. Zhang, J. Evers, and S.-Y. Zhu, Phys. Rev. Lett. 110, 033901, (2013).
[23] J. Fujita, M. Levy, R. M. O. Jr, L. Wilkens, and H. Dötsch, Appl. Phys. Lett. 76, 2158 (2000).
[24] B. E. A. Saleh and M. C. Teich, Fundamentals of Photonics, 2nd ed (Wiley Interscience, Hoboken, N.J, 2007).
[25] D. Jalas, A. Petrov, M. Eich, W. Freude, S. Fan, Z. Yu, R. Baets, M. Popovi, A. Melloni, J. D. Joannopoulos, M. Vanwolleghem, C. R. Doerr, and H. Renner, Nat. Photonics 7, 579 (2013).
[26] R. Fleury, D. L. Sounas, C. F. Sieck, M. R. Haberman, and A. Alú, Science 343, 516 (2014).
[27] S. A. Cummer, Science 343, Issue 6170, pp. 495-496, (2014)
[28] N. A. Estep, D. L. Sounas, J. Soric, and A. Alú, Nat. Phys. 10, 923 (2014).
[29] L. D. Tzuang, K. Fang, P. Nussenzveig, S. Fan, and M. Lipson, Nat. Photonics 8, 701 (2014).
[30] K. Fang, Z. Yu, and S. Fan, Phys. Rev. Lett. 108, 153901 (2012).
[31] K. Fang, Z. Yu, and S. Fan, Nat. Photonics 6, 782 (2012).
[32] J.-H. Wu, M. Artoni, and G. C. La Rocca, J. Opt. Soc. Am. B 25, 1840 (2008).

Figures

FIG. 1: (Color online) Schematic of a spatiotemporally modulated photonic crystal with a static defect membrane at the center of the crystal. The right inset schematically shows reflection (R) and the place of localized mode for two different cases: (upper) no time modulation where the localized mode is reciprocal, (middle and lower) spatiotemporal modulation where the position of localized mode depends on the direction of the incident beam. The photonic crystal is formed (see the left inset) from a driven Rb atom-cell (Γ-type three-level system) with a standing wave field with detuning δ between the two components.

FIG. 2: (Color online) (a) Transmission (red) and reflection (blue) for the static and reciprocal photonic crystal ($\delta = 0$) with a defect in the middle of the lattice. The defect mode appears at the $\Delta_f \approx -0.13$MHz. (b,c) Left and right transmission and reflection for the space and time-modulated photonic crystal ($\delta = 0.015\gamma_{ab}$) with the defect in the middle of it. For the left (right) incident, b (c), the defect mode is appeared at the $\Delta_f \approx -0.38(-0.29)$MHz (see the insets), highlighted with a dash green (orange) line. The position of the dash line, shows that the frequency for which we have the defect mode for left (right) incident beam, the right (left) incident beam observes the bandgap (bandpass) and has zero (finite) transmission. The atomic parameters are $\gamma_{ab} = \gamma_{ac} = 6\times10^6 s^{-1}, \Omega_1 = 30\times10^6 s^{-1}, \Omega_2 = 25\times10^6 s^{-1}, N = 19^{19} m^{-3}$.

FIG. 3: (Color online). (a-c) Distribution of the field intensity for the zero detuning (a) at the defect mode, (b) in the passband window, and (c) in the gap. (d-f) Distribution of the field intensity for left incident beam when $\delta = 0.015\gamma_{ab}$ (d) at the defect mode $\Delta_f \approx -0.38$MHz, (e) in the passband window $\Delta_f \approx -0.29$MHz, and (f) at $\Delta_f \approx -0.155$MHz. (g-i) Distribution of the field intensity for the right incident beam when $\delta = 0.015\gamma_{ab}$ (g) at the gap $\Delta_f \approx -0.38$MHz, (h) at the defect mode $\Delta_f \approx -0.29$MHz, and (i) at passband with $\Delta_f \approx -0.155$MHz. Notice that the defect mode of the left incident beam is located at the gap for the right incident beam while the defect mode of the right incident beam is located at the passband and has a scattering feature.

FIG. 4: (Color online) Position of the defect mode vs. the detuning for the left (squares) and right incident (circles) beams. A Linear fit is depicted by a continuous line on top of the symbols. The splitting of the position of the modes shows a linear behavior similar to the Zeeman effect, showing the similarities between time-dependent modulated lattice and a magnetic biasing.

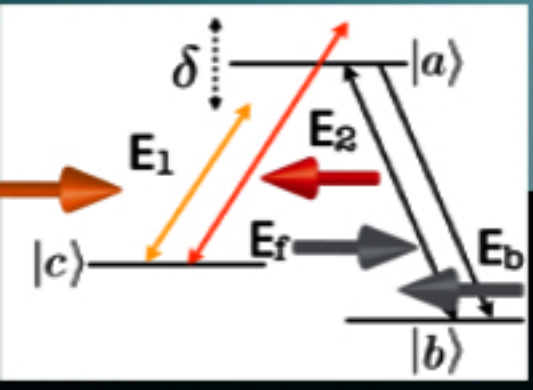
δ
|a⟩
E1
E2
Ef
Eb
|c⟩
|b⟩

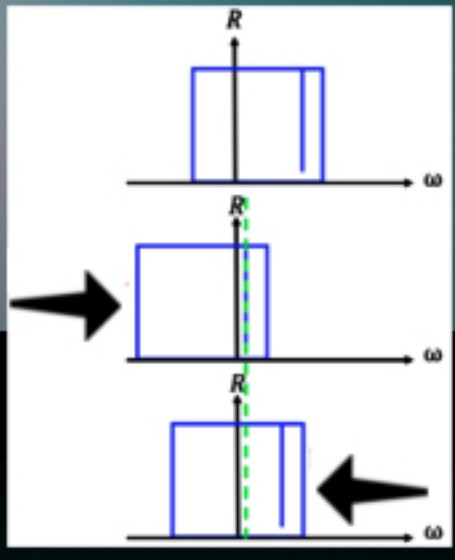
R
ω
R
ω
R
ω

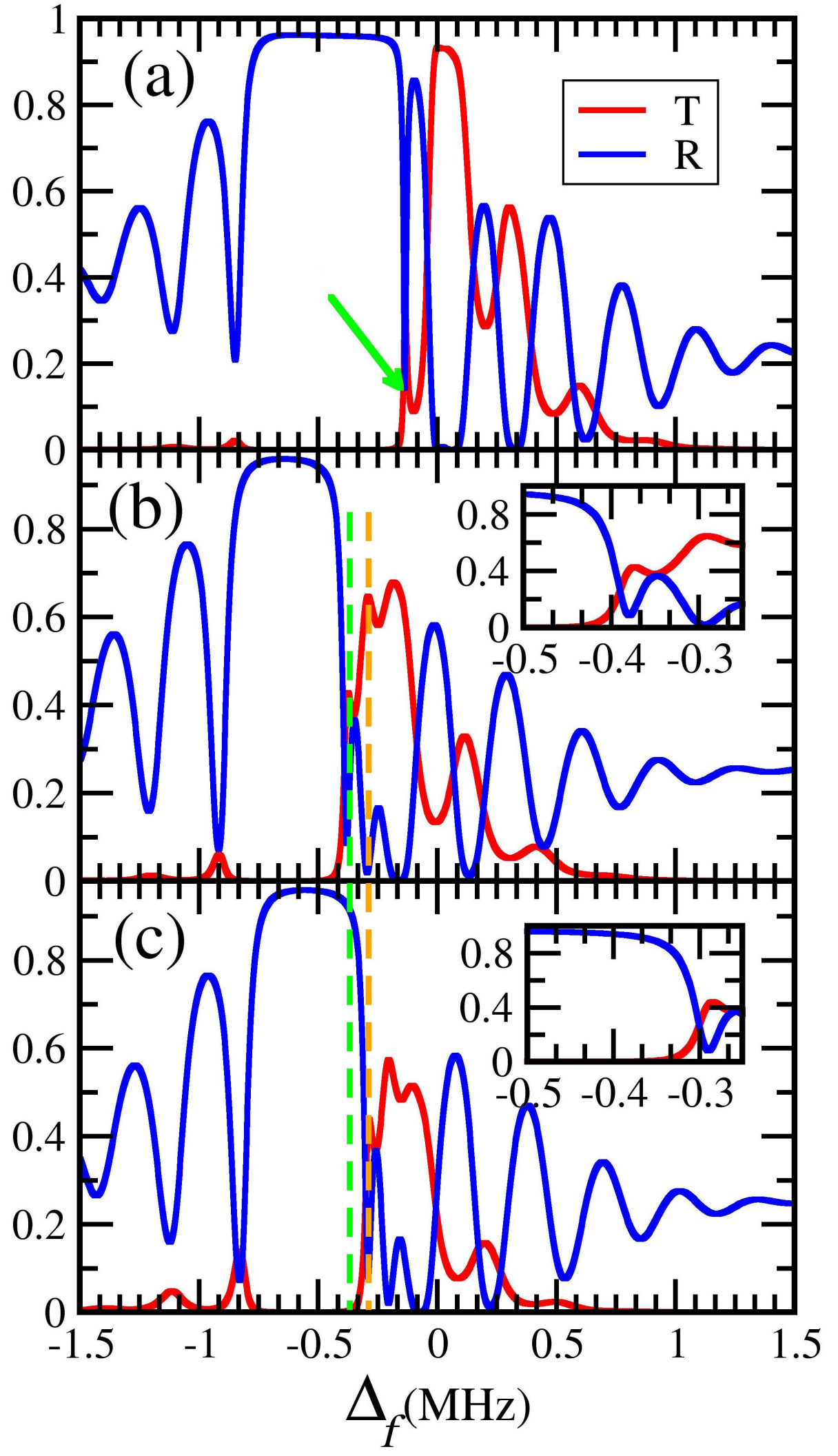
(a)
(b)
(c)
T
R
0
0.2
0.4
0.6
0.8
1
-1.5
-1
-0.5
0
0.5
1
1.5
-0.5
-0.4
-0.3
Δ_f(MHz)

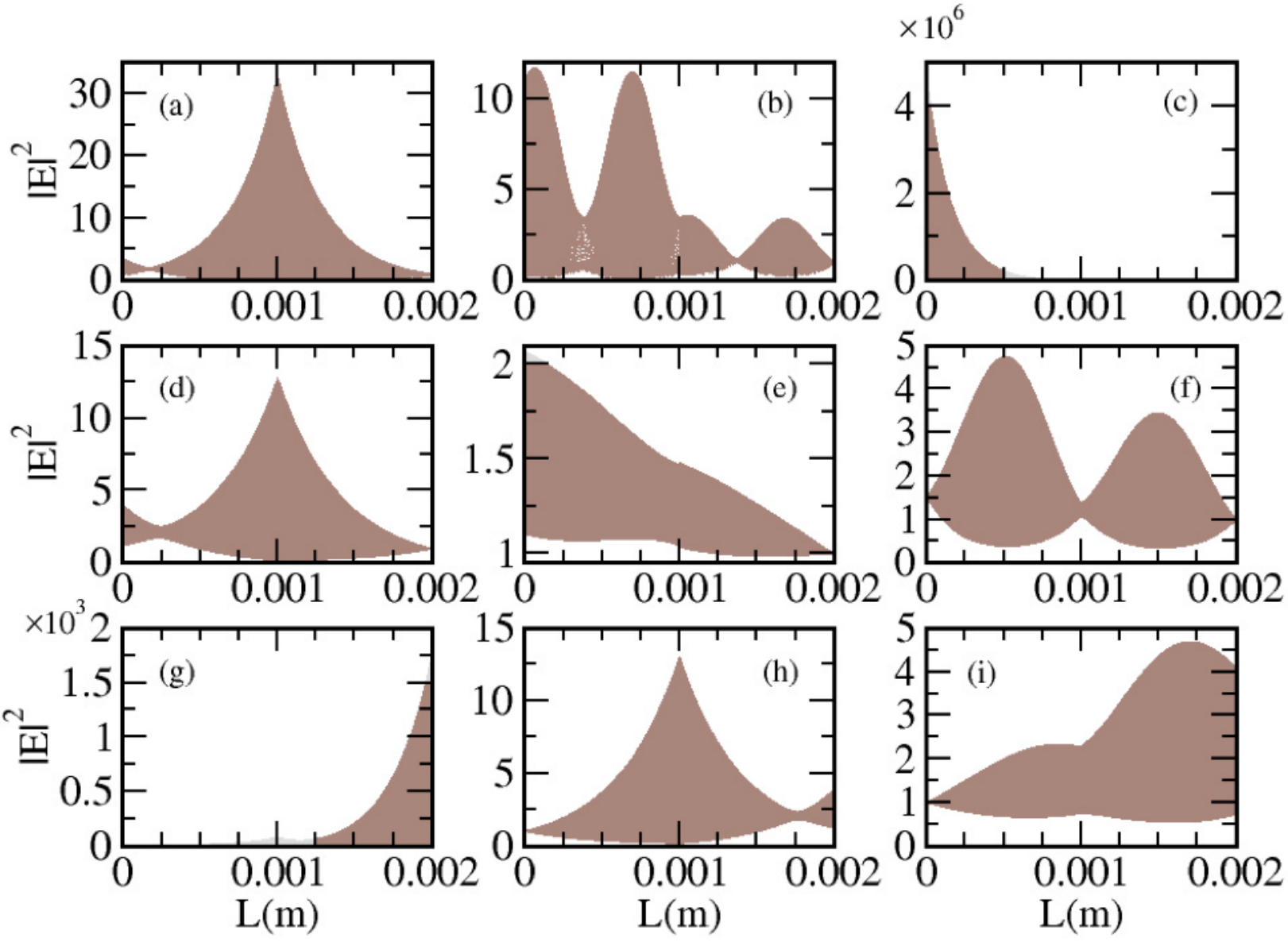
(a)
(b)
(c)
(d)
(e)
(f)
(g)
(h)
(i)
$|E|^2$
$\times 10^6$
$\times 10^3$
L(m)
0
0.001
0.002

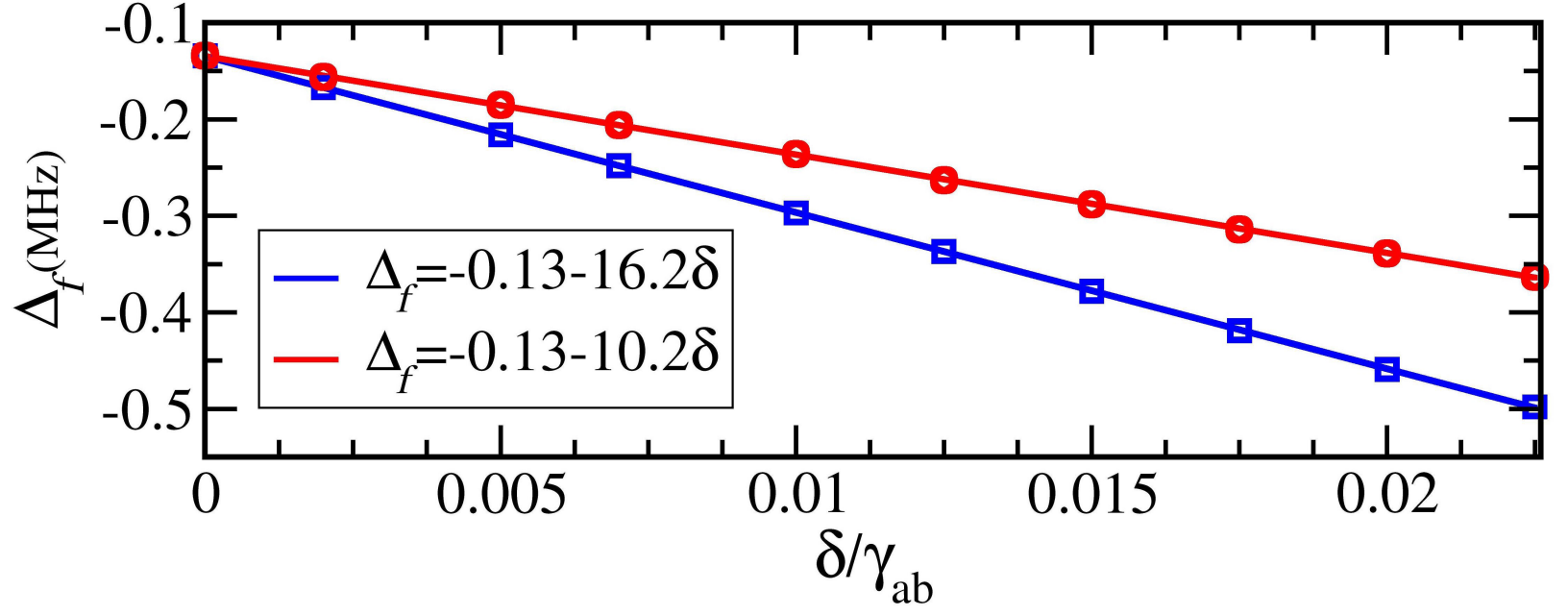
-0.1
-0.2
-0.3
-0.4
-0.5
Δ_f(MHz)
Δ_f=-0.13-16.2δ
Δ_f=-0.13-10.2δ
0
0.005
0.01
0.015
0.02
δ/γ_{ab}